2014 IEEE International Conference on Robotics & Automation (ICRA)
Hong Kong Convention and Exhibition Center
May 31 - June 7, 2014. Hong Kong, China

Design and Evaluation of a Parallel-Series Elastic Actuator for Lower Limb Exoskeletons*

Yanhe Zhu, *Member, IEEE*, Jixing Yang, Hongzhe Jin, Xizhe Zang and Jie Zhao, *Member, IEEE*

***Abstract*—This paper presented a novel compliant actuator used for lower limb exoskeletons. The compliant joint consists of a series elastic actuator (SEA) and parallel elastic (PE) unit. SEA has various advantages as the actuator of assistive exoskeletons, such as low output impedance, impact absorption, precise force control and high stability. We designed and fabricated a novel SEA as the primary joint actuator which is compact, adjustable and low-cost. Meanwhile an additional elastic unit is installed in parallel with the SEA to improve energy utilization by storing and releasing energy during motion cycles. An adaptive stable controller is designed to realize the joint following motion to a virtual limb. The algorithm can identify and compensate the undetermined contact stiffness between the joint output and the virtual limb. Finally, the performance of the actuator is evaluated through motion tracking and energy-conservation experiments. Preliminary results indicate the validity of the design and imply its potential usage in lower limb exoskeletons.**

I. Introduction

STUDY of powered human exoskeleton robot began in the late 1960s [1]. After decades of research, a variety of exoskeleton robots for human performance enhancement and rehabilitation have been developed. Some typical and successful examples of exoskeleton robots are the Berkeley Lower Extremity Exoskeleton(BLEEX) of the University of California, Berkeley [2], the Raytheon/Sarcos XOS exoskeleton suit of Raytheon company, the Hybrid Assistive Limb (HAL)-5 exoskeleton [3] of the University of Tsukuba and the rehabilitation robot Lokomat [4] which is used with the treadmill. All of these exoskeletons use traditional actuators, such as hydraulic actuators and motors.

However, because the exoskeleton robot should work with human, new compliant actuators that can insure the safety and comfort of the man-machine interaction have become one of current focuses of research. Series elastic actuator (SEA) [5], [6], by introducing elastic between the traditional actuator and the load, is a good solution to the above problem and has already been used in some exoskeletons.

Roboknee [7], actuated by a linear SEA, is a 1 DOF knee exoskeleton for enhancing strength and endurance during walking. User intent is determined through the knee joint angle and ground reaction forces. Torque is applied across the knee in order to allow the user's quadriceps muscles to relax. University of Twente has developed a gait rehabilitation exoskeleton, called LOPES [8]. Each leg of LOPES has three actuated rotational joints, which are actuated by Bowden cable based SEA. The joints are impedance controlled to allow bidirectional mechanical interaction between the robot and the training subject. The Wilmington Robotic Exoskeleton (WREX) [9] , is a gravity balanced upper limb orthosis for children with muscular weakness. In order to increase the range of joint motion of children, and to make the exoskeleton able to lift a substantial weight, series elastic actuators were attached to two joints of WREX. There are also many other series elastic actuators developed for exoskeleton, [10]-[12].

Continuous working time is a great challenge to mobile exoskeletons due to the capacity limitation of power source. To solve this problem, PE unit can be used to improve energy utilization by storing and releasing energy during motion cycles.

Although some articles have analyzed the effects of parallel-and series elasticity in an actuator, to the best of our knowledge, there are still no such prototypes been fabricated and tested.

This paper designed and fabricated a new type of exoskeleton compliant actuator by combining the SEA and the PE unit together. Part II introduces the work principle of the SEA and PE unit. Part III introduces the design process of the compliant actuator. In part IV, a control algorithm which has considered the change of the contact stiffness between human and exoskeleton is designed. Finally, the validity of the designed control algorithm and performance of the prototype are evaluated in part V.

II. Working Principle

A. Series elastic actuator

Series elastic actuator is a device with bionic characteristics, which introduces elastic element between the traditional actuator and the load. SEA has been applied in the human-machine interaction and walking robots, etc.

Series elastic actuator has the following characteristics: low output impedance, impact resistance ability, high force control precision and stability, capability of energy storage to improve the efficiency of the system [5]-[7].

Based on the above advantages, SEA is decided to be used in our design. The bevel gears are used to change the transmission direction. Schematic diagram of the designed SEA is shown in Figure 1.

*This work was supported by National High Technology Research and Development Program of China (863 Program) under Grant 2012AA041505 and National Natural Science Foundation of China (Grant No. 61004076).

Yanhe Zhu, Jixing Yang, Hongzhe Jin, Xizhe Zang, Jie Zhao are with the State Key Laboratory of Robotics and System, Harbin Institute of Technology.

Yanhe Zhu is the corresponding author(yhzhu@hit.edu.cn).

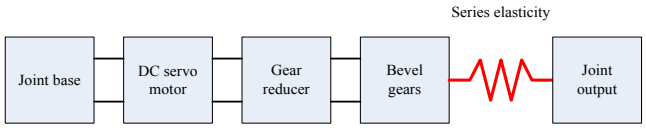

Fig 1 Schematic diagram of the series elastic actuator

B. *Parallel elastic unit*

Passive biped walking theory is proposed by the Canadian scholar McGeer in 1990s [13]. The core of passive walking is to improve the utilization efficiency of gravity potential energy by realizing the alternately transformation between the gravity potential energy and kinetic energy in the process of walking. In this paper, the principle of passive walking is used in the design of parallel elastic unit.

In order to analyze the process of energy transformation in the walking, simulations of human walking and the exoskeleton walking were realized with ADAMS and BRG.LifeMOD. Following are the exoskeleton joint power curves (Figure 2) and joint angle curves (Figure 3) in the sagittal plane.

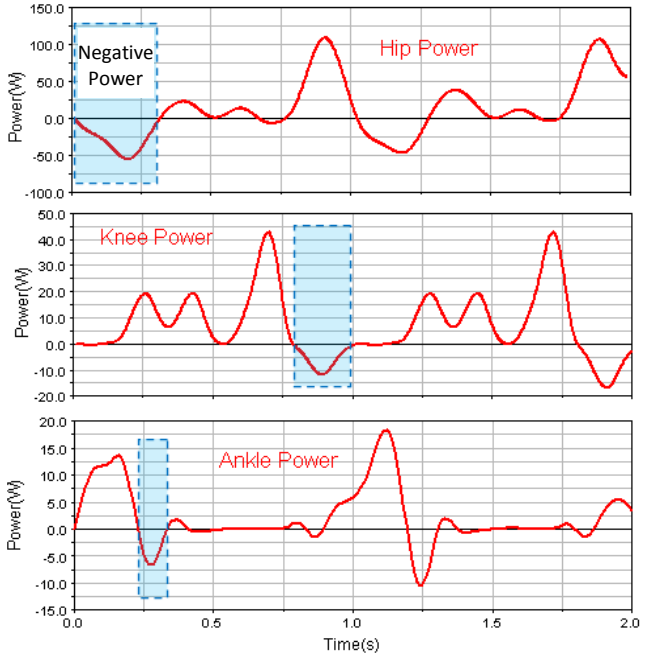

Fig 2 Exoskeleton joint power curves

As can be seen in Figure 2, in a gait cycle (about 1 second), there is a period for all the joints, when the joint power is negative. It can be seen from the hip joint angle curve in Figure 3 that the hip joint extends from 0 degree to the maximum extension angle, namely the support limb rotates from the vertical position to oblique position when the hip joint do negative work. In other words, gravity potential energy of the system reduces, when the hip joint do negative work.

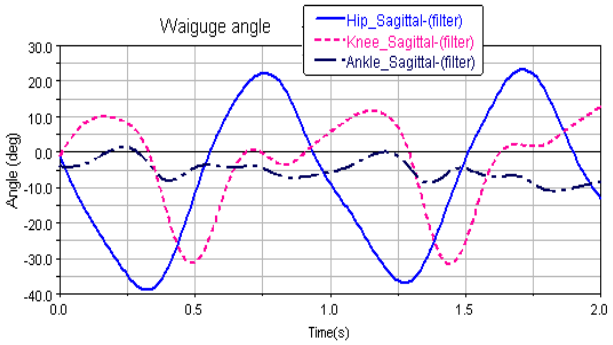

Fig 3 Exoskeleton joint angle curves

However, the motor can't store the reduced gravity potential energy, resulting in energy waste. Thus an energy saving project is proposed: During the negative work phase, by introducing conservative force components in the joint (such as a spring) to do work instead of the motor, gravitational potential energy could be transformed into elastic potential energy. By releasing the stored energy in positive work phase, the recycling of the gravity potential energy is achieved.

Although it can be taken as the energy recycling element, series elasticity generates output force executing directly on the driving motor, which will lead to considerable electrical energy consuming. Therefore, pure passive spring in parallel with the joint is used to store the gravitational potential energy and improve energy utilization.

III. Device Design

A compact joint with a SEA and a PE unit is designed. The CAD model of the joint is shown in Figure 4. A brushless DC servo motor is chosen as the power source. The motor is connected with the encoder and the output shaft of the motor is connected with a planetary gear reducer. The motor and the joint base are placed in parallel, reducing the lateral width of the exoskeleton, but this configuration needs to introduce an additional mechanism to change the transmission direction by 90 degree. This paper uses a pair of bevel gears whose reduction ratio is 3:1. The big bevel gear is fixedly connected to plate 1 by pins and screws and the plate 2 is fixedly connected to the joint shaft. Series elasticity is placed between the plate 1 and plate 2, whose concrete structure will be introduced in the following.

Figure 5 is the internal structure of the joint: plate 2 is connected with the joint shaft by key and will transfer torque to the shaft; joint shaft is connected with joint output link by a cylindrical pin. In addition, an angle sensor is mounted on the joint shaft inside the joint: the sensor casing is fixed to the joint shaft by a sleeve and the sensor output shaft is fixed to the joint base through the end cover.

A. *Design of the SEA*

The designed series elasticity is shown in Figure 6. Disk spring is used as the elastic element between the plate 1 and

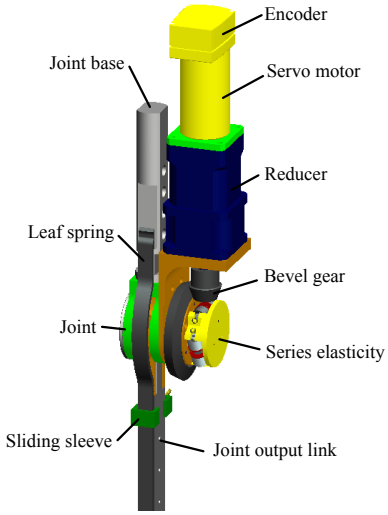

Fig 4 CAD model of the joint

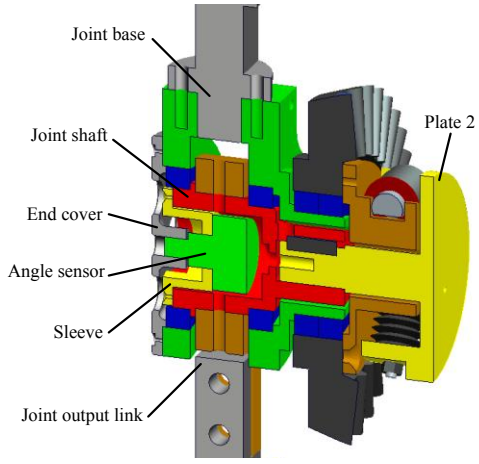

Fig 5 Internal structure of the joint

plate 2. Disk spring has the characteristics of small size, high rigidity and high stability. A plurality of disk springs in series composes disk spring group, whose rigidity is inversely proportional to the number of disk springs and can be adjusted by change of the number of the disk springs. The design here uses three groups of disk springs evenly distributed on the circumference of plate 2. The relative rotation between plate 1 and plate 2 will compress the spring groups and the elastic forces of the springs generate a pure torque.

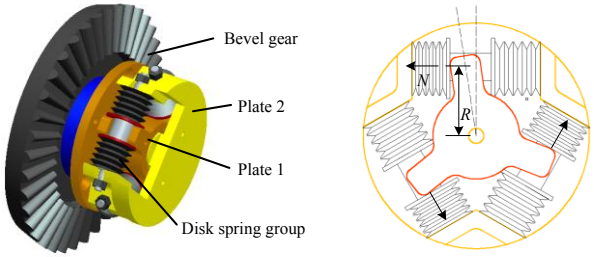

Fig 6 Series elasticity

According to the need of the exoskeleton, stiffness design principle of the disk springs is that the angle difference of plate 1 and plate 2, $\theta_m = 10°$, for the transfer of maximum torque.

According to the exoskeleton simulation results, considering the effect of friction, we assume that the maximum joint torque $T = 50\text{N}\cdot\text{m}$. The arm of spring force N is $R = 20\text{mm}$.

When the maximum torque is transferred, the spring force N is:

$$N = \frac{T}{3R} = \frac{50}{3\times 0.02}\text{N} = 833\text{N} \quad (1)$$

Due to the rotation angle is very small, change of the transmission radius is ignored. Thus the compression of disk spring group is:

$$\delta = R\tan\theta_m = 20\times\tan 10° = 3.5\text{mm} \quad (2)$$

Disk spring stiffness is:

$$K = N/\delta = 238\text{N/mm} \quad (3)$$

Each spring group contains 10 disk springs and stiffness of each spring is 2380N/mm.

B. Design of the PE unit

According to the previous analysis, the PE unit here is only designed for the hip joint. The elastic element used in the PE unit is a leaf spring. One end of the spring is connected with the output link of the joint and the other end is in a free state and can just contact with the joint base when the joint is in the $0°$ position. By adjusting the position of sliding sleeve, the stiffness of the spring can be changed to adapt to different loads. The CAD model of the PE unit is shown in Figure 4.

The process of energy storage and release of the PE unit can be equivalent to the process shown in Figure 7: From state A to state B, center of gravity of the system goes down and the spring is bended for the sake of gravity, namely the gravitational potential energy is transformed into elastic potential energy. From state B to state C, the joint stretches and the leaf spring releases the stored energy. From state C to state D, the leaf spring is separate from the joint base and the PE unit doesn't work.

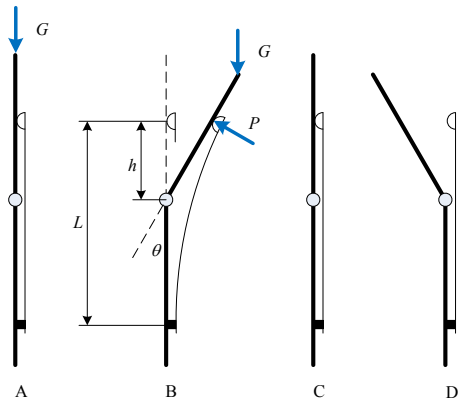

Fig 7 Process of energy storage and release

In order to reduce the force generated by the motor, the torque produced by the parallel spring should be as similar as possible to the load torque changed with joint angle. According to the simulation results, the hip torque relative to the joint angle changes approximately in a linear growth from 0, when the exoskeleton hip joint do negative work. The following is a validation of the similarities between the elastic torque of the spring and the exoskeleton required torque.

Firstly, the finite element analysis of the leaf spring bending deformation is done, as shown in Figure 8. 65Mn is selected as the spring material, whose elastic modulus *E*=200Gpa, Poisson's ratio is 0.3. Analysis results show that, the deflection of the leaf spring is proportional to the force at the end of the spring, which means that the spring can be analyzed as a simple straight rod.

Installation dimension of the leaf spring, *h*, *L*, and the force between spring and exoskeleton, *P* are shown in Figure 7. So the torque generated by the spring is:

$$T \approx P\frac{h}{\cos\theta} = \frac{3EIh^2}{L^3}\cdot\frac{\sin\theta}{\cos^2\theta} \tag{4}$$

The above I is the moment of inertia of the leaf spring cross-section. From the formula, it is known that in $-30°\sim 0$, the elastic moment and the joint angle have approximately linear relationship, which coincides with the exoskeleton joint torque in the negative work phase.

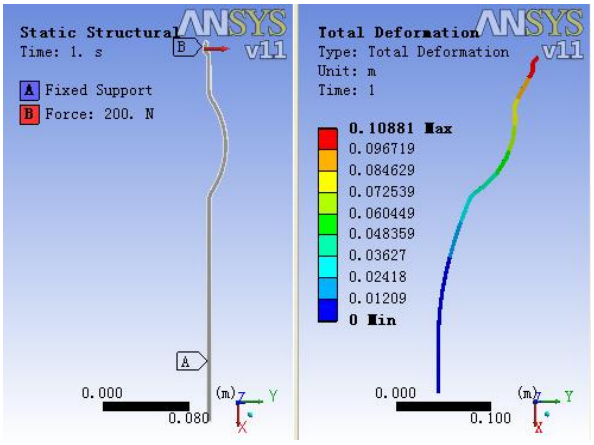

Fig 8 Finite element analysis of the leaf spring

IV. Control Method

For exoskeleton, following the human position is the foundation to realize the walking assistance.

In this paper, the position deviation between human leg and the exoskeleton is changed into force signal. Follow motion of human leg is accomplished by controlling the contact force between the exoskeleton and human body.

In order to realize the precise control of the contact force, this paper adopts an adaptive stable algorithm, [14], [15], for the exoskeleton robot joint, which is based on inner velocity loop PI controller with desire force feedforward and is applied to estimate the contact stiffness between the exoskeleton and human body.

The contact stiffness between human and the exoskeleton is $k(t)$; the contact flexibility is $\lambda(t)=1/k(t)$; the force measuring point on the exoskeleton is $x_e(t)$; the force measuring point on the human leg is $x_h(t)$; the contact force between the exoskeleton and leg is $f(t)$. We can get the following formula:

$$x_e(t)=\lambda(t)f(t)+x_h(t) \tag{5}$$

The velocity loop PI controller with desire force feedforward is:

$$\dot{x}_d(t)=\tilde{\lambda}(t)\dot{f}_d(t)-K_f\Delta\dot{f}(t)-I_f\Delta f(t) \tag{6}$$

In the above formula, $\dot{x}_d(t)$ is the desired exoskeleton speed, f_d is the desired contact force, $\Delta f(t)=f(t)-f_d(t)$, $\tilde{\lambda}(t)$ is estimated value of $\lambda(t)$, K_f, I_f are the coefficients of PI controller. Here, $f_d\neq 0$, which means that the exoskeleton needs to help people overcome gravity.

The following iterative algorithm is used to identify the contact flexibility online:

$$\dot{\tilde{\lambda}}(t)=-\alpha\dot{f}_d(t)\Delta f(t),\alpha>0 \tag{7}$$

This algorithm makes the control law adaptive to the stiffness change between human and exoskeleton, which ensures that better force control can be achieved. Control system block diagram is shown in Figure 9.

It can prove that the system is stable, if we have the condition, $\lim_{t\to\infty}\Delta\dot{x}(t)=\lim_{t\to\infty}[\dot{x}_e(t)-\dot{x}_d(t)]=0$, according to the articles [14], [15].

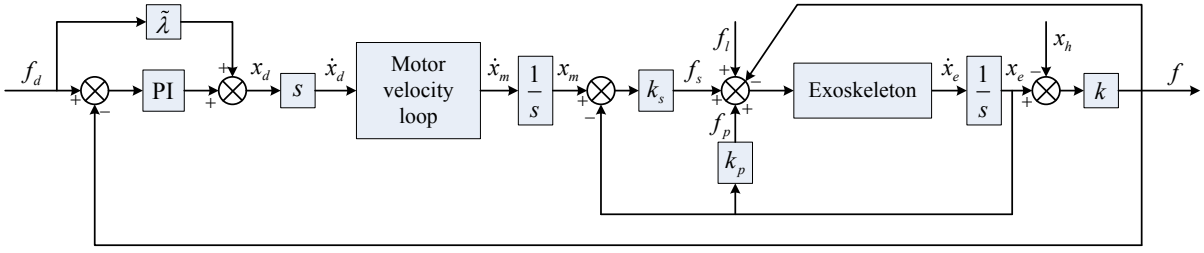

Fig 9 Control system block diagram

V. Experimental Results and Analysis

A. Test platform

Test platform for the actuator is shown in Figure 10. A PC-104 microcomputer is selected as the host computer. The Elmo Simple-IQ driver is chosen for PWM control of the motor. RS232 serial port communication is used between the driver and the host computer. In addition, a PCM-3718 A/D acquisition card is added for the acquisition of the signals from a joint angle sensor, a pressure sensor and a precision resistance. A brushless servo motor whose rated power is 400W and rated speed is 3000r/min, is selected as power source. A 2500P/r incremental encoder and a planetary gear reducer with the 20:1 transmission ratio are attached to the motor.

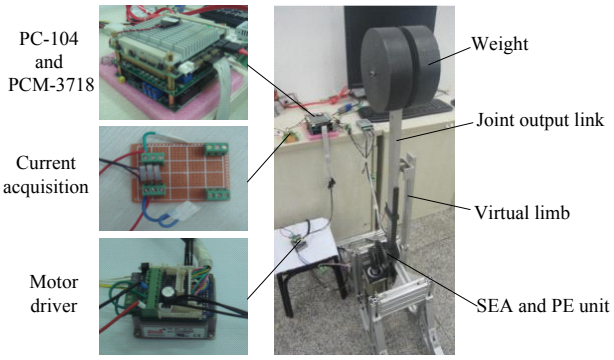

Fig 10 Test platform

B. Motion tracking test

A motion tracking test is done without the PE unit. The swing of a virtual limb, instead of human leg，is used as input signal of the test. A position deviation sensor is set between the virtual limb and output link of the joint. The controller designed above is used to carry out the test.

Figure 11 shows the structure and working principle of the position error sensor, which converts position information to pressure information through the combination of two symmetric compression springs and a piece of pressure sensor. Springs in the sensor are pre compressed at zero error position. When there is position deviation between the virtual limb and the exoskeleton, the spring is stretched or compressed, causing the change of pressure sensor output. The sensor pressure range is 0-4.5N and the output voltage, which is proportional to the pressure, has a range of 0-5V.

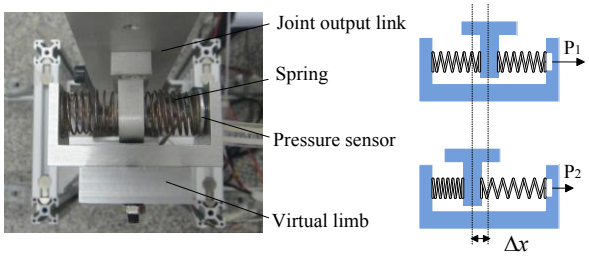

a) Structure of the sensor b) Working principle of the sensor

Fig 11 Position error sensor

The experimental results are shown in Figure 12. Figure 12-a) and 12-b) are respectively the exoskeleton joint angle curve and angular velocity curve in the position tracking experiment. It can be seen that the movement of the joint is stable and there is no local oscillation in the test process. Figure 12-c) is a pressure curve from pressure sensor in the process of experiment. The spring pre pressure is 0.8N and the maximum pressure deviation is 0.7N, which means that the resistance force between the leg and joint is very small. Considering the stiffness of the spring is 0.15N/mm, the maximum position deviation is 4.67mm. According to the distance from the installation position of the sensor to the joint axis, which is 300mm, it is clear that the maximum angle deviation is 0.89 degree.

From the analysis on the experimental results, we can draw the conclusion: precise position tracking can be acquired based on the designed control method above.

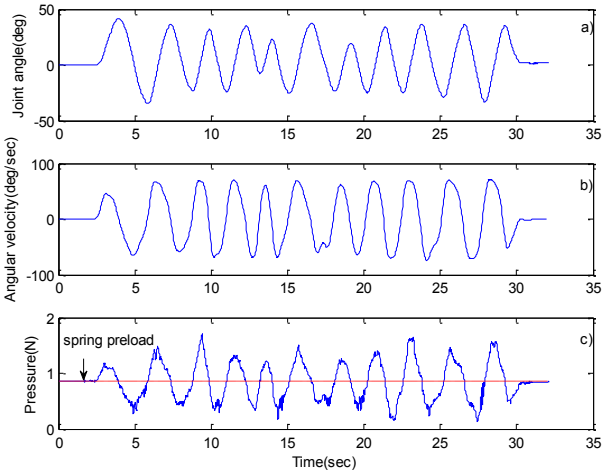

Fig 12 Experimental results of position tracking test

C. Energy-conservation test

In order to verify the energy-conservation effect of the PE unit, the motion test with load is needed. In this test, the joint is placed upside down and the joint load is simulated by a 10 kg weight installed at the end of the joint output link. The energy-conservation effect of the PE unit can be proved by the comparison of power consumption of the test with or without the PE unit. In the test, the joint angle is controlled by the simulated joint angle from ADAMS.

The energy-conservation test is only for the hip joint of the exoskeleton. From part III, we know that, the leaf spring will separate from the joint base, when the joint angle is bigger than $0°$, which is not associated with energy saving, so this experiment contains only the part in which the joint angle is $-30° \sim 0°$.

The joint torque created by the weight is:

$$T = G'L' \sin\theta \tag{8}$$

Among the formula (8), G' is the gravity of the weight, L' as the distance from center of gravity to the joint axis and θ is the joint angle. The torque produced by the weight is corresponding to the joint load torque, for $\sin\theta$ varies

approximately linearly with θ, when θ changes from –30° ~ 0° .

The motor's total power can be calculated through the acquisition of input voltage (48V) and current of the motor. The current is acquired by measure the voltage across a precise resistance.

The joint swung 100 cycles with or without the leaf spring respectively. Figure 13 shows the power curve of a cycle. The solid line represents the motor power consumption of test without the leaf spring and the dashed represents the motor power consumption of test with the leaf spring. Changed from 18W to 7W, the motor peak power is reduced by 60%. Average of the energy integrated from the power of the 100 cycles is 3.82J without PE unit and 1.85J with PE unit, which means adding the leaf spring saves 52% energy .

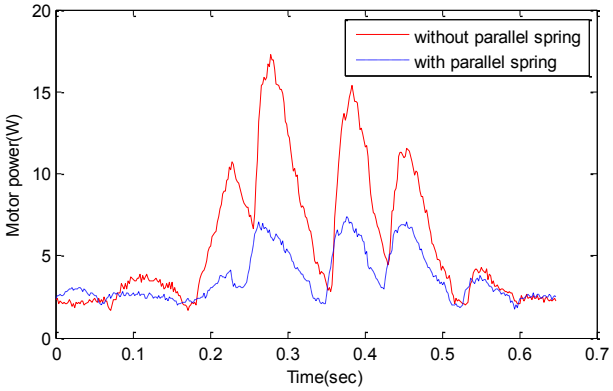

Fig 13 Power of motor with and without the PE unit

As can be seen, the power consumption of the joint is significantly reduced with the PE unit.

The energy-conservation effect of PE unit is successfully validated by the experimental results, but the measured motor power has large fluctuation. Considering the used joint control method for this parallel-series elastic actuator is only stable, but not optimal, further research on the joint control method is needed to reduce the fluctuation of the motor power.

As the elastic force of the PE unit has not fully fit the joint torque, there still has space for improvement in the energy-conservation effects.

VI. CONCLUSION

This paper designed and evaluated a novel compliant actuated joint used for lower limb exoskeletons, which consists of a series elastic actuator and parallel elastic unit.

1) A parallel-series elastic actuator is designed. Instead of special designed components, three groups of low-cost disk springs are used to form a compact series elasticity. A parallel elastic unit, consisting of a leaf spring and a sliding sleeve, is designed for improving the system energy utilization with different loads.

2) An adaptive stable algorithm based on inner velocity loop PI controller with desire force feedforward, is proposed for the joint control. Then, the performance of the actuator is evaluated through motion tracking and energy-conservation experiments.

Preliminary results imply its potential usage in lower limb exoskeletons. Further research on the joint control method and performance improvement is needed.

ACKNOWLEDGEMENTS

This work is supported by National Hi-tech Research and Development Program of China(Grant #2012AA041505) and National Natural Science Foundation of China (Grant No. 61004076). The authors express gratitude for the financial support.

REFERENCES

[1] Aaron M. Dollar, Hugh Herr, "Lower Extremity Exoskeletons and Active Orthoses: Challenges and State-of-the-Art," *IEEE Transactions on Robotics*, vol. 24, no. 1, pp. 144-158, 2008.

[2] Adam B. Zoss, H. Kazerooni, and Andrew Chu, "Biomechanical Design of the Berkeley Lower Extremity Exoskeleton (BLEEX)," *IEEE/ASME Transactions on Mechatronics,* vol. 11, no. 2, pp. 128-138, 2006.

[3] Yoshiyuki Sankai, "HAL: Hybrid Assistive Limb Based on Cybernics," *Springer Tracts in Advanced Robotics,* vol. 66, n STAR, pp. 25-34, 2010.

[4] S. Jezernik, G. Colombo, T. Keller et al, "Robotic Orthosis Lokomat: A Rehabilitation and Research Tool," *Neuromodulation: Technology at the Neural Interface*, vol. 6, no. 2, pp: 108-115, 2003.

[5] Gill A. Pratt, Matthew M. Williamson, "Series Elastic Actuators," in *IEEE International Conference on Intelligent Robots and Systems*, vol. 1, pp. 399-406, 1995.

[6] David William Robinson, "Design and Analysis of Series Elasticity in Closed-loop Actuator Force Control," Ph.D. dissertation, Mechanical Engineering., Massachusetts Institute of Technology, 2000.

[7] Jerry E. Pratt, Benjamin T. Krupp, Christopher J. Morse et al, "The RoboKnee: An Exoskeleton for Enhancing Strength and Endurance During Walking," in *Proceedings - IEEE International Conference on Robotics and Automation*, vol. 2004, no. 3, pp. 2430-2435, 2004.

[8] Jan F. Veneman, Rik Kruidhof, Edsko E. G. Hekman et al, "Design and Evaluation of the LOPES Exoskeleton Robot for Interactive Gait Rehabilitation," *IEEE Transactions on Neural Systems and Rehabilitation Engineering,* vol. 15, no. 3, pp. 379-386, 2007.

[9] Daniel Ragonesi, Sunil Agrawal, Whitney Sample et al, "Series Elastic Actuator Control of a Powered Exoskeleton," in *Proceedings of the Annual International Conference of the IEEE Engineering in Medicine and Biology Society*, EMBS, pp. 3515-3518, 2011.

[10] Claude Lagoda, Alfred C. Schouten, Arno H. A. Stienen et al, "Design of an electric Series Elastic Actuated Joint for robotic gait rehabilitation training," *2010 3rd IEEE RAS and EMBS International Conference on Biomedical Robotics and Biomechatronics, BioRob 2010*, pp. 21-26, 2010.

[11] Kyoungchul Kong, Joonbum Bae, Masayoshi Tomizuka, "A Compact Rotary Series Elastic Actuator for Human Assistive Systems," *IEEE/ASME Transactions on Mechatronics*, vol. 17, no. 2, 2012.

[12] Fabrizio Sergi, Dino Accoto, Giorgio Carpino et al, "Design and Characterization of a Compact Rotary Series Elastic Actuator for Knee Assistance During Overground Walking," in *Proceedings of the IEEE RAS and EMBS International Conference on Biomedical Robotics and Biomechatronics*, pp. 1931-1936, 2012.

[13] Tad MacGeer, "Passive Dynamic Walking,", *International Journal of Robotics Research*, vol. 9, no. 2, pp. 62-82, 1990.

[14] Jaydeep Roy, Louis L. Whitcomb, "Adaptive Force Control of Position/Velocity Controlled Robots: Theory and Experiment," *IEEE Transactions on Robotics and Automation*, vol. 18, no. 2, pp. 121-137, 2002.

[15] Yanhe Zhu, Xizhe Zang, Jihong Yan, "Transparent haptic interaction for admittance type haptic interfaces," *Journal of Harbin Institute of Technology* (in Chinese), vol. 41, no. 3, pp: 22-25, 2009.